International Journal of Research and Technology in Electrical Industry

journal homepage: ijrtei.sbu.ac.ir

Shahid Beheshti University

Finite time thrust vector tracker based on a new smooth second-order adaptive sliding mode controller

Mohammad Asadi[1], Vahid Behnamgol[*2,], Ahmadreza Vali[3]

[1]Iran University of Science and Technology, Tehran, Iran

[2] Energy Research Centre, Damavand Branch, Islamic Azad University, Tehran, Iran

[3] Electrical and Computer Engineering Department, Malek Ashtar University of Technology

ARTICLE INFO

Article history:
Received 20 February 2024
Revised: 16 May 2024
Accepted: 29 May 2024

Keywords:
Thrust vector control
Second order sliding mode
Chattering
Finite-time stability
Adaptive gains.

ABSTRACT

This paper introduces a novel adaptive second-order sliding mode algorithm for finite-time control of uncertain nonlinear systems. Traditional first-order sliding modes are hindered by chattering and dependence on the upper bound of uncertainty. Although adaptive sliding modes with dynamic gains remove the need for this upper bound, they still suffer from chattering and lack finite-time stability. The proposed algorithm incorporates an additional term in the control law, ensuring a smooth control signal, eliminating chattering, and achieving finite-time stability of the closed-loop system. This method is applied to a thrust vector-based flying object for pitch angle tracking amidst aerodynamic coefficient uncertainties and environmental disturbances. The performance of the proposed thrust vector system is demonstrated through computer simulations, comparing it with two other adaptive first-order and an adaptive super-twisting sliding mode methods. Simulation results show significant improvements in control performance, including reduced chattering and enhanced stability, underscoring the practical effectiveness of the proposed method.

1. Introduction

The aim of the control system in flying objects is to stabilize the object and execute the commands generated by the guidance system. This system includes control sensors, a controller (or control logic), and servomechanism. Thrust vector control (TVC) is a specific method to control the position and attitude of the flying object, and, in some missions, only this method can be applied. TVC is a critical technology in aerospace engineering, enabling precise maneuverability and stability of rockets and aircraft by directing the thrust from their engines. Traditional TVC methods often involve mechanical systems, such as gimbals and nozzles, to deflect the exhaust flow and control the vehicle's attitude. Recent advancements have introduced fluidic thrust vectoring techniques, which use secondary fluid flows to manipulate the primary exhaust stream, offering benefits like reduced weight and complexity. These innovations enhance control effectiveness, especially in modern military applications where agility and stealth are paramount tips. Despite these advancements, challenges

* Corresponding author
E-mail address:
vahid_behnamgol@damavandiau.ac.ir
http://dx.doi.org/10.48308/ijrtei.2024.235765.1046

remain in optimizing TVC systems for various flight conditions and ensuring reliable performance under dynamic loads [1, 2]. The thrust vector control system is used when the air density is low to produce high maneuver acceleration and quick change of the flight path, which increases the efficiency of the control system [3, 4]. This type of control system has been used [5] for interceptor interception and [6, 7] for adjusting the satellite position. The nonlinear equations of the motion for the longitudinal axis of an interceptor based on thrust vector control are presented [8], which include uncertainty in some parameters, such as aerodynamic coefficients. Due to uncertainties, it is necessary to use robust controllers to ensure high tracking accuracy.

One of the most well-known and powerful methods for increasing the robustness and quick convergence properties of non-linear systems is sliding mode control [9]. The sliding mode method is widely used in the control of nonlinear, especially in flight control systems [10], interceptor guidance [11], integrated guidance and control systems [12] , and quadrotor AUVs trajectory control [13]. But the first-order sliding mode has two fundamental problems: a) to determine the gain k in the first-order sliding mode, we need the upper bound of system uncertainties; b) in first-order sliding mode control law, the sign function, which is an uneven function, appears directly in control law and leads to chattering in the control signal [14]. This phenomenon causes high-frequency switching, which is one of the obstacles to applying to real systems and can even lead to instability.

Recent advancements in sliding mode control have significantly enhanced its applicability and performance in various engineering fields. To get rid of the upper bound of system uncertainties, one of the most famous methods is the use of adaptive sliding mode (ASMC) [15]. In this method, the gain of k changes with the increase of uncertainty. But in addition to the fact that this method still suffers from chattering, the finite time stability of this method is not guaranteed, which has been achieved in first-order sliding mode.

To fix chattering, one solution is to use approximation methods, such as using the saturation function [16] or tanh function [17, 18] instead of the sign function. However, these methods limit the sliding paths to the adjacent paths instead of the sliding surface, which reduces the tracking accuracy and the system's robustness [19]. One of the most powerful methods to reduce the chattering effect is the high-order sliding mode method (HOSMC). This approach reduces the chattering by reducing the sliding variable and its derivatives to zero [20]. The main challenge of this method is that higher derivatives of the sliding variable are needed. Also, the finite-time stability of this method has been done by using geometric approaches, and mathematical algorithms such as Lyapunov analysis are not able to guarantee the finite-time stability of this method [21]. Super twisting sliding mode (ST), which is one of the second-order sliding mode (SOSMC) algorithms, only needs the sliding variable itself, while the rest of the second-order sliding mode algorithms also need the derivative of the sliding variable [22, 23]. However, this algorithm still includes a discrete function, so the control signal is not completely smooth.

To conclude, recent advancements in sliding mode control have significantly enhanced its applicability and performance in various engineering fields. One notable development is the integration of higher-order sliding modes, which offer improved robustness and accuracy by reducing chattering effects [24]. Additionally, adaptive sliding mode control techniques have been introduced, allowing systems to dynamically adjust control parameters in response to changing conditions [25]. These methods have shown promise in applications ranging from robotics to power electronics, where precise control is crucial. Despite these advancements, challenges remain in ensuring stability and performance under diverse and unpredictable conditions.

Reducing chattering in sliding mode control continues to be a significant area of research, with numerous strategies suggested to lessen its negative impacts. Although approximation techniques might affect system performance, second-order sliding mode control appears, promising to produce smoother control signals. Nonetheless, ensuring finite-time stability and convergence time remains a challenge. In this paper, the control signal is smooth due to the inclusion of a second-order term, and the sliding mode gain is adaptively adjusted. Additionally, this paper completely addresses the issue of finite-time stability.

This paper is presented to achieve the following goals: a) presenting a comprehensive model of a thrust vector-based interceptor; b) designing a new smooth adaptive second-order sliding mode with the aim of tracking the pitch angle of the interceptor-based thrust vector in the presence of system uncertainties, that the generated control signal is smooth and without chattering, and the calculation of gain k does not need the upper bound of uncertainty; c) Ensuring finite-time stability of closed-loop system using Lyapunov analysis and achieving convergence time.

The structure of the paper is as follows. In the second section, the dynamic model of the thrust vector-based interceptor is presented. In the third section, the first smooth adaptive second-order sliding mode is introduced, and after that, the control law is presented for the thrust vector-based interceptor. Then, in the fourth section, the simulation results are presented, and the performance of the methods is compared with each other. Finally, the conclusion is expressed.

2. Thrust vector-based interceptor dynamic model

In this section, the dynamics of an interceptor's pitch channel, which is controlled based on the change of the thrust vector, is expressed. The thrust vector control system is used in many solid and liquid fuel interceptors. The interceptor can fly in the right position using a thrust vector control system [26, 27]. The body, velocity, and ground coordinates are necessary for the mathematical analysis of the interceptor motion equations. The basis of these coordinates for the interceptor is the center of gravity. In the ground coordinates, X_g and Z_g are on a horizontal plane, and Y_g is on a vertical plane. In body coordinates, the X_b axis coincides with the line that passes through the center of the interceptor and represents the roll axis. Z_b axis is perpendicular to X_b in the horizon plane and represents the pitch axis. Y_b axis, which also represents the yaw axis. Body coordinates are fixed relative to the interceptor and move with it. In the velocity coordinate, X_V is in the direction of the interceptor velocity [28].

The pitch plane is the $X - Y$ surface, the yaw plane is the $X - Z$ surface, and the $Y - Z$ surface is the roll plane. Ground coordinates and body coordinates are related by angles (ϕ, θ, ψ). Ground coordinates and velocity coordinates are related by angles (γ, σ). The velocity coordinates and the body coordinates are related in the pitch plane by the angle of attack (α) and in the yaw plane by the lateral slip angle (β). The relationship between the velocity and body coordinates is obtained:

$$\begin{bmatrix} X_b \\ Y_b \\ Z_b \end{bmatrix} = \begin{bmatrix} \cos(\beta)\cos(\alpha) & \cos(\beta)\sin(\alpha) & -\sin(\beta) \\ -\sin(\alpha) & \cos(\alpha) & 0 \\ \sin(\beta)\cos(\alpha) & \sin(\beta)\sin(\alpha) & \cos(\beta) \end{bmatrix} \times \begin{bmatrix} X_V \\ Y_V \\ Z_V \end{bmatrix} \quad (1)$$

The angles between the different coordinates are shown in figure (1) to (3).

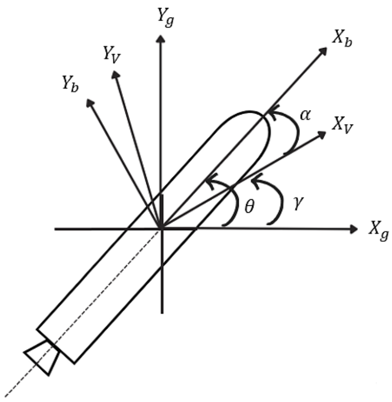

Fig 1: Angles in the pitch plane

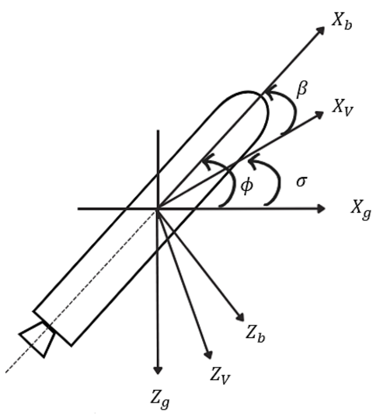

Fig 2: Angles in the yaw plane

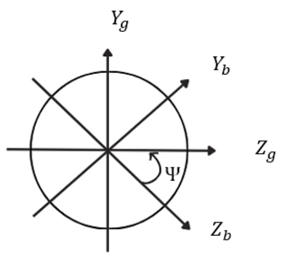

Fig 3: Angles in the roll plane

Also, the axes of the body and velocity coordinate system, along with moments, forces, and other quantities, are shown in figure (4).

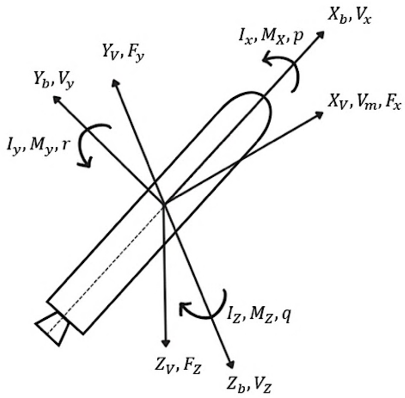

Fig 4: moments, forces, and other quantities in the velocity and body axis system

For an interceptor, the equations of motion are obtained as follows [8, 29]:

$$F_x = m\dot{V}_m \quad (2)$$
$$F_y = m\dot{V}_m\dot{\gamma} \quad (3)$$
$$F_z = -mV_m\cos(\gamma)\dot{\sigma} \quad (4)$$
$$M_x = I_x\dot{p} - (I_y - I_z)\mathrm{rq} \quad (5)$$
$$M_y = I_y\dot{r} - (I_z - I_x)\mathrm{qp} \quad (6)$$
$$M_z = I_z\dot{\mathrm{q}} - (I_x - I_y)\mathrm{pr} \quad (7)$$
$$\dot{X} = V_m\cos(\gamma)\cos(\sigma) \quad (8)$$
$$\dot{Y} = V_m\sin(\gamma) \quad (9)$$
$$\dot{Z} = -V_m\cos(\gamma)\sin(\sigma) \quad (10)$$
$$\dot{\phi} = (\mathrm{r}\cos(\psi) - \mathrm{q}\sin(\psi))/\cos(\theta) \quad (11)$$
$$\dot{\theta} = \mathrm{r}\sin(\psi) + \mathrm{q}\cos(\psi) \quad (12)$$
$$\dot{\psi} = \mathrm{p} - \tan(\theta)(\mathrm{r}\cos(\psi) - \mathrm{q}\sin(\psi)) \quad (13)$$
$$\dot{\alpha} = \dot{\theta} - \dot{\gamma} \quad (14)$$
$$\dot{\beta} = \dot{\gamma} - \dot{\sigma} \quad (15)$$

In these equations, M_x, M_y and M_z are moments $[N.m]$, F_x, F_y and F_z are forces $[N]$, I_x, I_y and I_z are moments of inertia $[kg.m^2]$, p, q and r are angular velocities $[rad/sec]$, X is the range of the interceptor $[m]$, Z is the horizontal displacement of the interceptor $[m]$, Y is the height of the interceptor $[m]$ and m is the mass of the interceptor $[kg]$. In an interceptor, forces and moments are generated by gravity, aerodynamics, and thrust. These forces and moments are presented as follows [28, 30]:

$$F_x = Tcos(\alpha - \delta_\alpha) - cos(\beta - \delta_\beta) - QS(C_{x0} + Cx(\alpha^2 + \beta^2)) - mgsin(\gamma) \quad (16)$$

$$F_y = T\,sin(\alpha - \delta_\beta) + QSC_y\alpha - mg\,cos(\gamma) \quad (17)$$

$$F_z = -T\,cos(\alpha - \delta_\alpha)\,sin(\beta - \delta_\beta) - QSC_z\beta \quad (18)$$

$$M_x = DQSm_{x0}\frac{\mathrm{p}D}{2V_m} \quad (19)$$

$$M_y = -T\,cos(\delta_\alpha)\,sin(\delta_\beta)X_{cg} + DQS\left(m_{y\beta} + m_{y\beta} + m_{y0}\frac{\mathrm{r}D}{v_m}\right) \quad (20)$$

$$M_z = T\,sin(\delta_\alpha)X_{cg} + DQS\left(m_{z\alpha} + m_{z0}\frac{\mathrm{q}D}{V_m}\right) \quad (21)$$

In these equations, m_{x0}, $m_{y\beta}$, m_{y0}, $m_{z\alpha}$ and m_{zo} are aerodynamic moments coefficients, C_x, C_{x0}, C_y and C_z are aerodynamic force coefficients, S is the area of the reference surface $[m^2]$, D is the maximum value of the body diameter [m], Q is the Dynamic pressure $[kg/m.sec^2]$, δ_α is the pitch nozzle deflection angle $[deg]$, δ_β is the yaw nozzle deflection angle $[deg]$, T is the thrust force $[N]$, X_{cg} is the distance between the nozzle and the center of mass $[m]$, and g is the gravity acceleration constant. By simplifying the equations of motion, the nonlinear equations in the pitch channel are expressed as follows [8]:

$$\begin{aligned}\dot{\theta} &= q\\ \dot{q} &= \frac{QSDm_{z\alpha}}{I_z}\alpha + \frac{QSD^2m_{z0}}{I_zV_m}\omega_z + \frac{TX_{cg}}{I_z}sin(\delta_\alpha)\\ \dot{\alpha} &= -\frac{QSC_y}{mV_m}\alpha - \frac{T}{mV_m}sin(\alpha - \delta_\alpha) + q + \frac{g}{V_m}cos(\theta - \alpha)\end{aligned} \quad (22)$$

There are two types of disturbances in the above equations:

- The disturbance caused by the interference of other channels appears as the term d_1 in the $\dot{\theta}$ equation.
- The disturbance caused by the wind appears as the term d_2 in the equations and affects the system in the opposite direction of the interceptor's velocity (V_m).

Considering the approximation $sin(\delta_\alpha) = \delta_\alpha$ and the mentioned disturbances, the interceptor state equations will be expressed as follows [31]:

$$\begin{aligned}\dot{\theta} &= q + d_1\\ \dot{q} &= \frac{QSD(m_{z\alpha})}{I_z}\alpha + \frac{QSD^2(m_{z0})}{I_z(V_m - d_2)}\omega_z + \frac{TX_{cg}}{I_z}\delta_\alpha\\ \dot{\alpha} &= -\frac{QS(C_y)}{m(V_m - d_2)}\alpha - \frac{T}{m(V_m - d2)}sin(\alpha - \delta_\alpha) + q + \frac{g}{V_m - d2}cos(\theta - \alpha)\end{aligned} \quad (23)$$

3. Control system design

In this section, firstly, the principles proposed by smooth adaptive second-order sliding mode control theory are stated, and then the considered controller is applied to an interceptor based on the thrust vector dynamic model presented in the previous section.

3.1. Smooth adaptive second-order sliding mode

Consider the following nonlinear system:

$$\dot{x} = f(x) + g(x)u + d(t) \quad (24)$$

Where $x \in X \subset \mathbb{R}^n$ is the state variables vector, $u \in \mathbb{R}$ is the input vector, and $f(x) \in \mathbb{R}^n$ is the vector of nonlinear functions. To describe the controller, it is assumed:

The sliding variable is expressed as $s = s(x,t)$, so by establishing $s = s(x,t) = 0$, the system (24) will have a desirable dynamic behavior. $s = s(x,t) = 0$ is called the sliding variable, and after the system paths reach the sliding variable, the system will be in the sliding phase. The dynamics of the sliding variable will be as (25):

$$\dot{s} = \frac{\partial s}{\partial t} + \frac{\partial s}{\partial x}f(x) + \frac{\partial s}{\partial x}g(x)u = a(x,t) + b(x,t)u \quad (25)$$

The ratio of sliding variable dynamics to the control input u is equal to one, and also, the internal dynamics are stable.

- The function $b(x,t)$ is definite, and the function $a(x,t)$ is indefinite, and is presented as follows:

$$a(x,t) = \bar{a}(x,t) + d(t) \quad (26)$$

According to (26), the sliding variable dynamics can be rewritten as follows:

$$\dot{s} = \bar{a}(x,t) + d(t) + b(x,t)u \quad (27)$$

Where $\bar{a}(x,t)$ is the definite part and $d(t)$ is the indefinite part of $a(x,t)$. We also assume that the uncertainty has an upper boundary in the form $|d| \leq L_d$. The controller u must be designed in such a way that the sliding variable $s = s(x,t)$ reaches zero and maintains it in the presence of uncertainty $d(t)$ in a finite period of time. For this purpose, the standard sliding mode control is introduced in (28):

$$u = \frac{1}{b(x,t)}[-\bar{a}(x,t) - ksign(s)] \quad (28)$$

Where $k = L_d + \eta$ is considered. To check the finite time stability of the sliding variable, we first consider the function $V = \frac{1}{2}s^2$, which is a positive definite function, as a Lyapunov candidate. To guarantee the finite time convergence of the sliding variable, the condition:

$$\dot{V} = \frac{\partial V}{\partial s}\dot{s} = s\dot{s} \leq -\eta|s| \quad (29)$$

Must be established, where η is a positive constant. By integrating (29), we will have:

$$t_r \leq \frac{|s(0)|}{\eta} \quad (30)$$

Therefore, the convergence time of the sliding variable can be calculated from the equation (30) and can be adjusted by changing the value of the parameter η. In order to calculate the gain k without requiring an upper bound on system uncertainties, the adaptive sliding mode control input is presented as follows:

$$u = \frac{1}{b(x,t)}\left(-\bar{a}(x,t) - \hat{k}(t)sign(s)\right)$$
$$\dot{\hat{k}}(t) = k_0|s| \qquad (31)$$
$$k_0 > 0$$

By placing control input (31) in (24) we will have the following:

$$\dot{s} = -\hat{k}(t)sign(s) + d(t)$$
$$\dot{\hat{k}}(t) = k_0|s| \qquad (32)$$

If we place $k = L_d + \eta$ in (28), the control input of the first-order sliding mode becomes as follows:

$$u_{SMC} = \frac{1}{b(x,t)}(-\bar{a}(x,t) - L_d sign(s) - \eta sign(s)) \qquad (33)$$

By comparing the above control law that guarantees finite time stability and the (31) control law, It can be said that in the first order sliding mode method, the term $L_d sign(s)$ is responsible for robustness in presence of uncertainty and the term $\eta sign(s)$ is responsible for ensuring the finite time stability of the sliding variable. But in the adaptive method, there is only a robust term, and the control input lacks a specific term to guarantee the finite time stability. Hence, a new smooth adaptive second-order sliding mode control law is presented as follows:

$$u = \frac{1}{b(x)}\left(-\bar{a}(x) - \mu|s|^{\gamma}\hat{k}sign(s) + u_s\right)$$
$$\dot{\hat{k}} = k_0(|s| + \mu|s|^{\gamma+1}) \qquad (34)$$
$$\dot{u}_s = -|u_s|s - \left(\hat{k}|s| + P\right)sign(u_s)$$

Where $0 < \gamma < 1, P > 0, \mu > 0$. so, the dynamics of a closed-loop system is obtained as follows:

$$\dot{s} = d(t) - \mu|s|^{\gamma}\hat{k}sign(s) + u_s$$
$$\dot{\hat{k}} = k_0(|\sigma| + \mu|s|^{\gamma+1}) \qquad (35)$$
$$\dot{u}_s = -|u_s|s - \left(\hat{k}|s| + P\right)sign(u_s)$$

Adding to the control law not only makes it possible to prove the finite time stability but also reduces chattering due to its dynamics and provides the second-order sliding mode behavior for the system. To check the stability of the system (34), we consider the candidate Lyapunov function in the following form:

$$V = \frac{1}{2}s^2 + \frac{1}{2k_0}(\hat{k} - L_d)^2 + |u_s| \qquad (36)$$

By deriving the above function, we will have:

$$\dot{V} = S\left(d(t) - \mu|s|^{\gamma}\hat{k}sign(s) + u_s\right) \qquad (37)$$

$$= sd(t) - \mu|s|^{\gamma+1}\hat{k} + u_s s + \hat{k}|s| - L_d|s| + \hat{k}\mu|s|^{\gamma+1} - L_d\mu|s|^{\gamma+1} - u_s s - \hat{k}|s| - P$$
$$= sd(t) - L_d|s| - L_d\mu|s|^{\gamma+1} - P \le -P$$

So, the finite time stability of the sliding variable s and $\hat{k} - L_d$ and u_s is guaranteed. It should be noted that the control input proposed in relation (34) has a smoother control signal due to the use of the $\mu|s|^{\gamma}\hat{k}sign(s)$ instead of $\hat{k}sign(s)$ that was used in the adaptive sliding mode.

3.2. Thrust vector control based on the proposed controller

Taking into account the uncertainties of the system, the dynamic equations of the interceptor will be as follows:

$$\dot{\theta} = q + d_1$$
$$\dot{q} = \frac{QSD(\overline{m_{z\alpha}} + \Delta m_{z\alpha})}{I_z}\alpha + \frac{QSD^2(\overline{m_{z0}} + \Delta m_{z0})}{I_z(V_m - d_2)}q + \frac{TX_{cg}}{I_z}\delta_\alpha \qquad (38)$$
$$\dot{\alpha} = -\frac{QS(\overline{C_y} + \Delta C_y)}{m(V_m - d_2)}\alpha - \frac{T}{m(V_m - d_2)}sin(\alpha - \delta_\alpha) + q + \frac{g}{V_m - d_2}cos(\theta - \alpha)$$

Here the object is to control the pitch angle. First, the system error is defined as follows:

$$e = y - y_d = \theta - \theta_d \qquad (39)$$

The sliding variable is defined as follows:

$$s = \dot{e} + \lambda e \qquad (40)$$

By deriving from the sliding variable, we will have:

$$\dot{s} = \ddot{e} + \lambda\dot{e} = \frac{QSD(\overline{m}_{z\alpha} + \Delta m_{z\alpha})}{I_z}\alpha + \frac{QSD^2(\overline{m}_{z0} + \Delta m_{z0})}{I_z(V_m - d_2)}q + \frac{TX_{cg}}{I_z}\delta_\alpha + \lambda q + \lambda d_1 + \dot{d}_1 \qquad (41)$$

According to (27), the values of $\overline{a}(t)$, and $b(t)$ will be as follows:

$$\overline{a}(t) = \frac{QSD(\overline{m}_{z\alpha})}{I_z}\alpha + \frac{QSD^2(\overline{m}_{z0})}{I_z}q + \lambda q$$
$$b(t) = \frac{TX_{cg}}{I_z}$$

And also:

$$d = \frac{QSD(\Delta m_{z\alpha})}{I_z}\alpha + \frac{QSD^2}{I_z}\left(\frac{\overline{m}_{z0} + \Delta m_{z0}}{V_m - d_2} - \overline{m}_{z0}\right) + \lambda d_1 + \dot{d}_1 \qquad (42)$$

Finally, according to (34), the control input will be as follows:

$$\delta_\alpha = \frac{1}{\frac{TX_{cg}}{I_z}}\left(-\frac{QSD(\overline{m}_{z\alpha})}{I_z}\alpha - \frac{QSD^2(\overline{m}_{z0})}{I_z}q - \lambda q - \mu|s|^\gamma \hat{k} sign(s) + u_s\right) \quad (43)$$

$$\dot{\hat{k}} = k_0(|s| + \mu|s|^{\gamma+1})$$

$$\dot{u}_s = -|u_s|s - (\hat{k}|s| + P)sign(u_s)$$

4. Simulation results

In this section, by showing the simulation results, the performance of the controller, which is designed in the previous section, is evaluated, and the proposed method (PM) is compared with the finite time adaptive sliding mode (FASMC) presented in [32] and the adaptive super-twisting sliding mode (ASTSMC) presented in [33]. In this research, the aim is to track the pitch angle (θ) of an interceptor based on the thrust vector. The initial value of the pitch angle is 40 degrees, and the goal is to bring it to 41 degrees. All simulations are done in MATLAB.

In (22), the dynamic model of the interceptor based on the thrust vector is presented. In this equation, some of the parameters change over time. During the flight, the mass of the interceptor decreases due to the burning of interceptor fuel. In general, the duration of the interceptor flight is divided into two parts.

Boost phase: at time 0-5.8 sec, and in this phase, the thrust force is maximum.

Sustain phase: at time 5.8-10 sec, and in this phase, the thrust force is minimum.

Variations of interceptor mass, thrust force, and interceptor velocity are shown in figures (5) to (7).

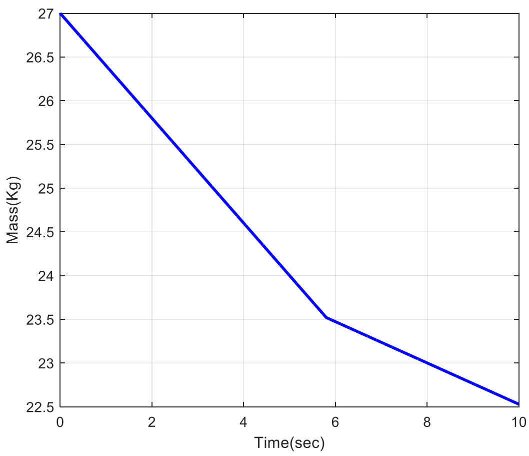

Fig 5: variation of the interceptor mass

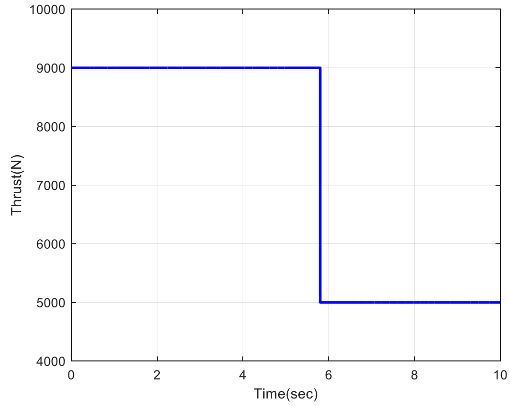

Fig 6: variation of the thrust force

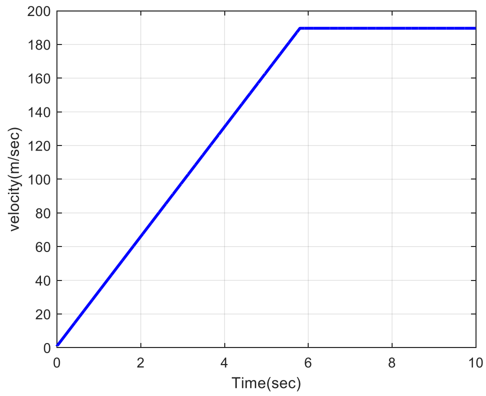

Fig 7: Variation of the interceptor velocity

Aerodynamic forces and torque coefficients in (22) also change with time. Variation of these parameters is shown in figures (8) to (10).

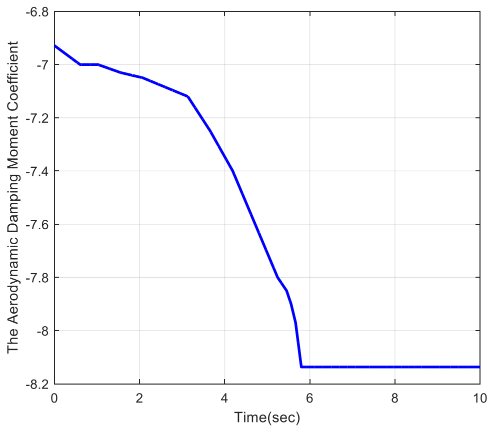

Fig 8: Aerodynamic damping moment coefficient ($\boldsymbol{m_{z0}}$)

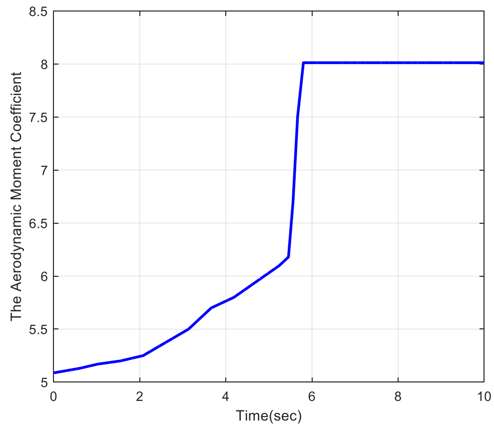

Fig 9: aerodynamic moment coefficient ($\boldsymbol{m_{z\alpha}}$)

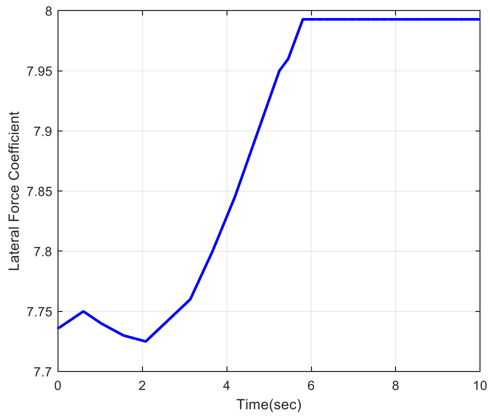

Fig 10: Lateral force coefficient ($\boldsymbol{C_y}$)

The disturbances in the system that were stated in the second section are also shown in figures (11) and (12).

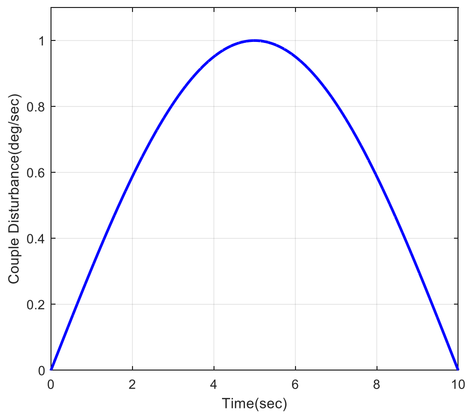

Fig 11: Disturbance caused by channel interference ($\boldsymbol{d_1}$)

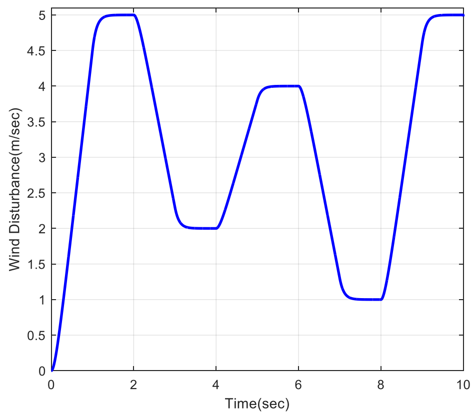

Fig 12: Wind disturbance ($\boldsymbol{d_2}$)

Based on the control laws presented in [34] and [33], the parameters used in them are considered as Tables (1) and (2).

Table 1: The parameters of the FASMC

Parameter	Value
λ	20
$\bar{K}_1$	4
$\bar{K}_2$	1
$\bar{K}_3$	0.5
τ	0.1

Table 2: Parameters of the ASTSMC

Parameter	Value
λ	20
ω_1	0.01
γ_1	1
ϵ	0.1
α_m	0.05
η	0.1
μ	0.7

The parameters of the proposed method are listed in Table (3).

Table 3: Parameters of the proposed method

Parameter	Value
λ	20
k_0	5
γ	0.3
μ	2
P	100

Figure (13) shows the comparison of the control inputs. As can be seen, there is severe chattering in the FASMC control signal and also the ASTSMC control signal is not completely smooth. But the input signal of the PM is completely smooth, and there is no chattering. In both PM and ASTSMC, the generated control signal is almost the same, and the amount of fin deflection in FASMC is significantly higher. Also, the pitch angle, the pitch rate, and the angle of attack are presented in figures (14), (15), and (16). The speed of pitch angle tracking in PM is higher than other methods.

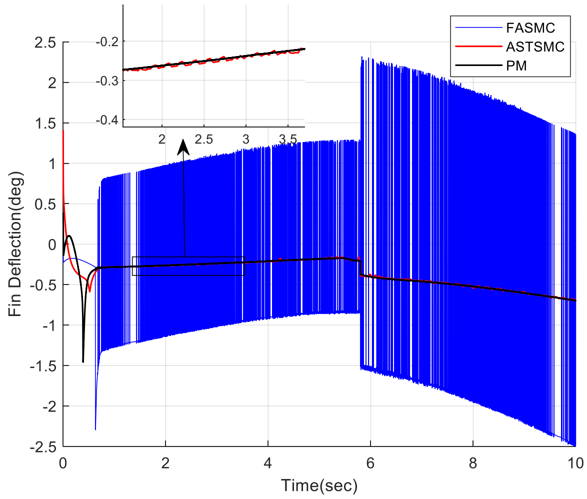

Fig 13: comparison of control inputs

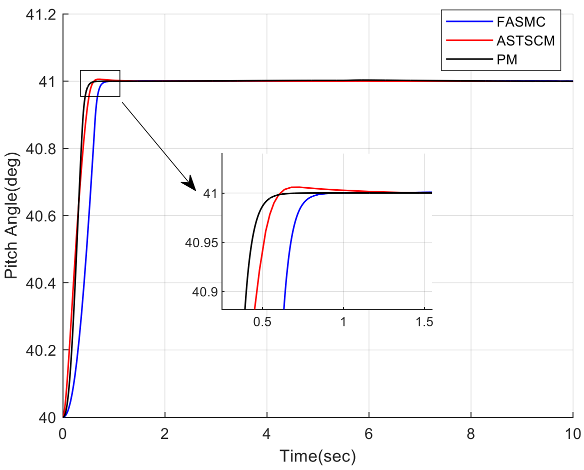

Fig 14: comparison of the pitch angle

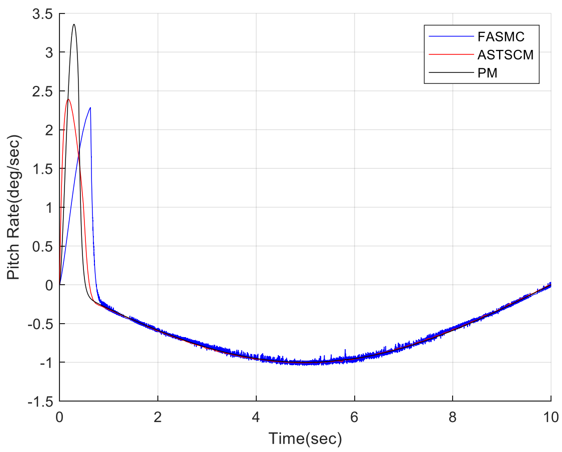

Fig 15: comparison of the pitch rate

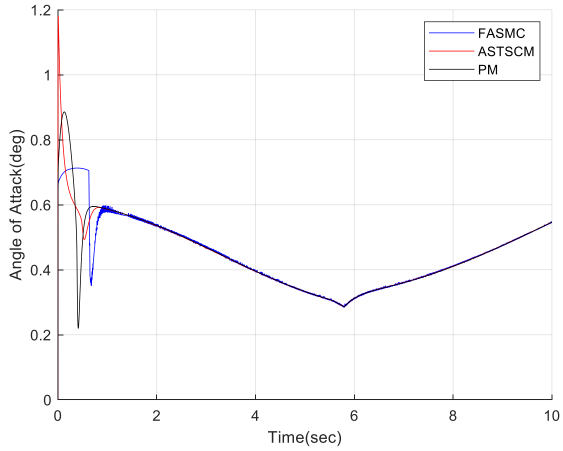

Fig 16: comparison of the angle of attack

To justify the output behavior of the system in the considered methods, the sliding variable is compared with each other in the figure (17). According to this figure, we can see that the speed of the sliding variable reaching zero is similar to the output tracking speed, and the PM sliding variable reaches zero faster. Also, the comparison of the adapted gain k along with the system uncertainty is shown in Figure (18). It is clear that all the methods have been able to overcome the uncertainties of the system well.

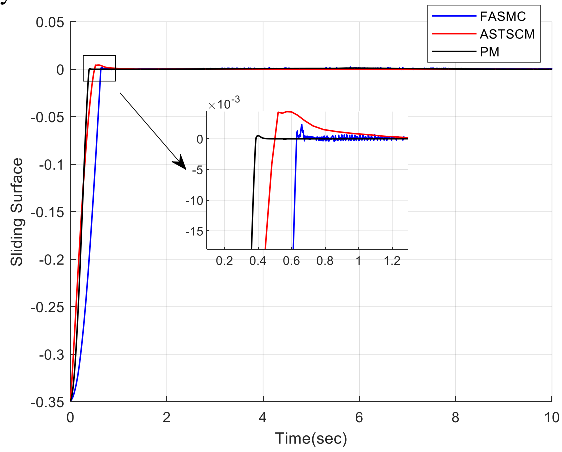

Fig 17: Comparison of sliding variable variation

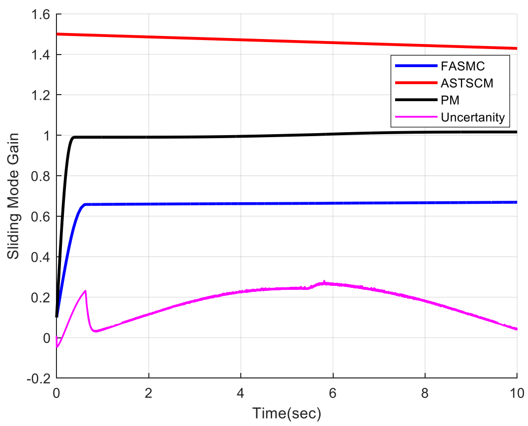

Fig 18: Controllers adaptive gain and uncertainty

5. Conclusion

A new smooth second-order sliding mode controller is proposed to track the pitch angle of a thrust vector interceptor. Due to its dynamic characteristics, the generated control signal is smooth, and by using the adaptive gains, the problem of needing to know the upper bound of uncertainty has been fixed. The finite time stability of the closed-loop system is proven using the Lyapunov algorithm. Simulation results show the effectiveness of the proposed control law in comparison with two other methods.

In conclusion, the advantages of the Proposed Method (PM) in comparison to two other methods are:

- Smooth Control Signal: The PM method eliminates chattering, providing a completely smooth control signal, unlike FASMC and ASTSMC.
- Improved Tracking Speed: The PM method achieves faster pitch angle tracking compared to other methods, enhancing the system's responsiveness.
- Effective Uncertainty Handling: The PM method, along with ASTSMC, effectively handles system uncertainties, ensuring robust performance

The proposed method involves many parameters, making it difficult to adjust each one for optimal results. Consequently, future research should consider using intelligent methods for parameter tuning.

6. References

[1] S. Afridi, T. A. Khan, S. I. A. Shah, T. A. Shams, K. Mohiuddin, and D. J. Kukulka, "Techniques of Fluidic Thrust Vectoring in Jet Engine Nozzles: A Review," *Energies,* vol. 16, no. 15, p. 5721, 2023.

[2] L. Sopegno, P. Livreri, M. Stefanovic, and K. P. Valavanis, "Thrust vector controller comparison for a finless rocket," *Machines,* vol. 11, no. 3, p. 394, 2023.

[3] X. Liu, Y. Zhang, W. Huang, and J. Wang, "Research of a fuzzy global sliding mode control scheme: A stability control scheme for anti-aircraft missile with swing nozzle thrust vector control," *Proceedings of the Institution of Mechanical Engineers, Part G: Journal of Aerospace Engineering,* vol. 229, no. 3, pp. 554-561, 2015.

[4] N. Wang, W. Lin, and J. Yu, "Sliding-mode-based robust controller design for one channel in thrust vector system with electromechanical actuators," *Journal of the Franklin Institute,* vol. 355, no. 18, pp. 9021-9035, 2018.

[5] F.-K. Yeh, "Adaptive-sliding-mode guidance law design for missiles with thrust vector control and divert control system," *IET control theory & applications,* vol. 6, no. 4, pp. 552-559, 2012.

[6] B. Xiao, Q. Hu, and P. Shi, "Attitude stabilization of spacecrafts under actuator saturation and partial loss of control effectiveness," *IEEE Transactions on Control Systems Technology,* vol. 21, no. 6, pp. 2251-2263, 2013.

[7] K. Lu, Y. Xia, Z. Zhu, and M. V. Basin, "Sliding mode attitude tracking of rigid spacecraft with disturbances," *Journal of the Franklin Institute,* vol. 349, no. 2, pp. 413-440, 2012.

[8] M. F. Ahmed and H. T. Dorrah, "Design of gain schedule fractional PID control for nonlinear thrust vector control missile with uncertainty," *Automatika,* vol. 59, no. 3-4, pp. 357-372, 2018.

[9] V. Behnamgol and A. R. Vali, "Terminal sliding mode control for nonlinear systems with both matched and unmatched uncertainties," *Iranian Journal of Electrical & Electronic Engineering,* vol. 11, no. 2, pp. 109-117, 2015.

[10] P. Ahmadi, A. Vali, and V. Behnamgol, "Autopilot Design Using Smooth Fractional Order Sliding Mode Control," 2018.

[11] V. Behnamgol, A. Vali, and A. Mohammadi, "A new observer-based chattering-free sliding mode guidance law," *Proceedings of the Institution of Mechanical Engineers, Part G: Journal of Aerospace Engineering,* vol. 230, no. 8, pp. 1486-1495, 2016.

[12] M. J. Rajabi, A. R. Vali, and V. Behnamgol, "Design of integrated Guidance and control system in the pitch channel using observer based chattering free sliding mode theory," *Journal of Control,* vol. 14, no. 1, pp. 49-63, 2020.

[13] I. Khabbazi and V. Behnamgol, "Fast Terminal Sliding Mode Controller for a Quadrotor Unmanned Aerial Vehicle," *Journal of Aerospace Science and Technology,* vol. 11, no. 1, pp. 37-45, 2018.

[14] Y. He, Y. Wu, and W. Li, "Nonlinear extended state observer-based adaptive higher-order sliding mode control for parallel antenna platform with input saturation," *Nonlinear Dynamics,* vol. 111, no. 17, pp. 16111-16132, 2023.

[15] B. Zhou, "Multi-variable adaptive high-order sliding mode quasi-optimal control with adjustable convergence rate for unmanned helicopters subject to parametric and external uncertainties," *Nonlinear Dynamics,* vol. 108, no. 4, pp. 3671-3692, 2022.

[16] V. Utkin, A. Poznyak, Y. Orlov, and A. Polyakov, "Conventional and high order sliding mode control," *Journal of the Franklin Institute,* vol. 357, no. 15, pp. 10244-10261, 2020.

[17] M. Xie, M. M. Gulzar, H. Tehreem, M. Y. Javed, and S. T. H. Rizvi, "Automatic voltage regulation of grid connected photovoltaic system using Lyapunov based sliding mode controller: a finite—time approach," *International Journal of Control, Automation and Systems,* vol. 18, pp. 1550-1560, 2020.

[18] G. V. BEHNAM and N. Ghahramani, "Design of a New Proportional Guidance Algorithm Using Sliding Mode Control," 2014.

[19] X. Liu and H. Yu, "Continuous adaptive integral-type sliding mode control based on

disturbance observer for PMSM drives," *Nonlinear dynamics,* vol. 104, pp. 1429-1441, 2021.

[20] J. Wang, Y. Hu, and W. Ji, "Barrier function-based adaptive integral sliding mode finite-time attitude control for rigid spacecraft," *Nonlinear Dynamics,* vol. 110, no. 2, pp. 1405-1420, 2022.

[21] V. Behnamgol, A. R. Vali, and A. Mohammadi, "A new adaptive finite time nonlinear guidance law to intercept maneuvering targets," *Aerospace Science and Technology,* vol. 68, pp. 416-421, 2017.

[22] A. Javadi and R. Chaichaowarat, "Position and stiffness control of an antagonistic variable stiffness actuator with input delay using super-twisting sliding mode control," *Nonlinear Dynamics,* vol. 111, no. 6, pp. 5359-5381, 2023.

[23] J. Liu, M. Sun, Z. Chen, and Q. Sun, "Super-twisting sliding mode control for aircraft at high angle of attack based on finite-time extended state observer," *Nonlinear Dynamics,* vol. 99, pp. 2785-2799, 2020.

[24] N. S. Gogani, V. Behnamgol, S. Hakimi, and G. Derakhshan, "Finite time back stepping supper twisting controller design for a quadrotor," *Engineering Letters,* vol. 30, no. 2, pp. 674-680, 2022.

[25] M. Ehsani, A. Oraee, B. Abdi, V. Behnamgol, and M. Hakimi, "Adaptive dynamic sliding mode controller based on extended state observer for brushless doubly fed induction generator," *International Journal of Dynamics and Control,* pp. 1-14, 2024.

[26] W. Sun, "Research on Thrust Vector/Aerodynamics Compound Control Method Based on Linear Quadratic Regulator Control for Solid Rocket," in *2020 Chinese Automation Congress (CAC)*, 2020: IEEE, pp. 545-548.

[27] L. Sopegno, P. Livreri, M. Stefanovic, and K. P. Valavanis, "Linear Quadratic Regulator: A Simple Thrust Vector Control System for Rockets," in *2022 30th Mediterranean Conference on Control and Automation (MED)*, 2022: IEEE, pp. 591-597.

[28] R. Bıyıklı, "Nonlinear dynamic inversion autopilot design for an air defense system with aerodynamic and thrust vector control," Middle East Technical University, 2022.

[29] J. R. Hervas and M. Reyhanoglu, "Thrust-vector control of a three-axis stabilized upper-stage rocket with fuel slosh dynamics," *Acta Astronautica,* vol. 98, pp. 120-127, 2014.

[30] J.-H. Hong and C.-H. Lee, "Nonlinear autopilot design for endo-and Exoatmospheric Interceptor with Thrust Vector Control," *IEEE Transactions on Aerospace and Electronic Systems,* vol. 56, no. 1, pp. 796-810, 2019.

[31] I. Martínez-Perez, R. Garcia-Rodriguez, M. Vega-Navarrete, and L. Ramos-Velasco, "Sliding-mode based Thrust Vector Control for Aircrafts," in *Proceedings of the 12th International Micro Air Vehicle Conference, Puebla, Mexico*, 2021, pp. 16-20.

[32] Y. Shtessel, F. Plestan, and C. Edwards, "Adaptive sliding mode and second order sliding mode control with applications: a survey," *IFAC-PapersOnLine,* vol. 56, no. 2, pp. 761-772, 2023.

[33] Y. Shtessel, M. Taleb, and F. Plestan, "A novel adaptive-gain supertwisting sliding mode controller: Methodology and application," *Automatica,* vol. 48, no. 5, pp. 759-769, 2012.

[34] F. Plestan, Y. Shtessel, V. Bregeault, and A. Poznyak, "New methodologies for adaptive sliding mode control," *International journal of control,* vol. 83, no. 9, pp. 1907-1919, 2010.